

STRUCTURAL, ENERGETIC AND ELECTRONIC PROPERTIES OF PURE/DOPED BN NANOTUBES

SIMONA RADA¹, IOAN SILAGHI DUMITRESCU¹

¹Departament of Chemistry, "Babeș-Bolyai" University, Cluj-Napoca, Ro-400084, Romania

ABSTRACT. The effects of chirality, length of tube, the influence of possible defects of atoms (due to deviations from the 1:1 stoichiometry or by the presence of other elements like aluminum or carbon) inside of single walled boron-nitride nanotubes on structural, energetic and electronic properties has been considered in this paper. The doping leads to thermodynamic instability of the armchair tubes. The chiral BN nanotubes can behave as a semiconductor or as an insulator depending on their chirality, diameter or length of tube whereas their analogues with armchair and zigzag geometry exhibit a constant band gap of 5-6eV.

1. Introduction

Experimental data and theoretical calculations have shown that carbon nanotubes¹ can behave either as a semiconductor or as a metal depending on their radius and chirality²⁻⁶, which is not desired in applications on nanodevices. The BN nanotubes may be good for possible applications in nanodevices because they have a constant band gap around 5,5eV independent of their diameter and chirality⁷⁻¹⁵.

Solids are characterized by a band structure in which the highest occupied band is called the valence band (*HOMO* orbital) and the lowest unoccupied band is called the conduction band (*LUMO* orbital). The energy difference between the bottom of the conduction band and the top of the valence band in a semiconductor or an insulator is called the band gap energy, E_g . The bandwidth of the band gap provides a distinction between a semiconductor and an insulator. When the band gap is not very large, usually ranging from 0,5 to 3,0eV, the material is a semiconductor, while an insulator has an $E_g > 3\text{eV}$,^{16, 17}.

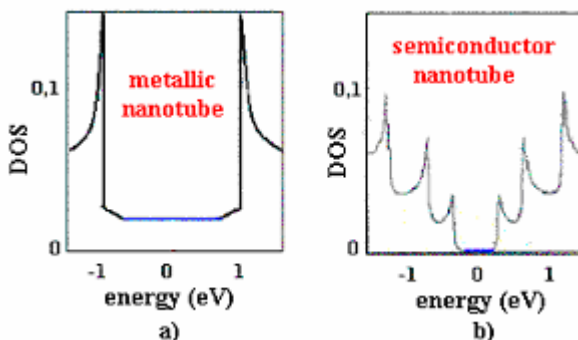


Figure 1. The density of states plots for metallic and semiconductor carbon nanotube^{18, 19, 20}.

Electrons in metals, semiconductors and insulators are described by the Bloch wave function. This function is a plane wave $e^{i\mathbf{k}\cdot\mathbf{R}}$ in the 3D space modulated by a function $\Phi_{\mathbf{k}}(x, y, z)$ having the periodicity of the crystal lattice in which the electrons move. According to Pauli exclusion principle no more than two electrons can found in the same Bloch wave function. The number of Bloch wave function states in the range of energies from E to $E + dE$ is called the density of states (DOS).

The shapes of the DOS plot for metallic and semiconductor nanotubes are shown in figure 1. The density of states at the Fermi energy is finite for a metallic tube and zero for a semiconductor tube.

The sharp peaks in density of states represent Van Hove singularities. They are typical for one-dimensional systems and dominate the density of states²⁰.

The aim of this study was to determinate the structural, energetic and electronic properties of the pure/doped boron nitride nanotubes. In order to examine these properties we explored theoretical models. The effects of chirality, length of tube, the influence of possible defects of atoms have been investigated. The electronic properties analysis has been carried out by density of states plots.

2. Methods of calculation

In this paper, various open ended single-walled BN nanotubes of the zigzag, armchair and chiral types, have been submitted to molecular-mechanics²¹ and semiempirical molecular orbital calculations²² (at AM1 and PM3 levels²³) using the HyperChem 4.5 and Spartan'02 software^{24, 25}.

To obtain the densities of state (DOS) of BN nanotubes, Hückel tight-binding calculations by BICON-CEDIT package²⁶ have been performed.

3. Results and discussion

A) Structural and energetic properties of BN nanotubes

The structures of the BN nanotubes with armchair, zigzag and chiral geometry^{27,28} were taken from reference²⁹. For the optimized structures at PM3 level, we found that the boron-nitrogen distances vary between 1,40 and 1,45Å, the B-N-B angles ranging from 112 and 120° and the N-B-N angles between 109 and 120°.

In the present work we have calculated the enthalpies of formation (ΔH) for a series of single-walled boron nitride nanotubes with zigzag ($n=5,6,7,\dots,14$), armchair ($n=m=5,6,7$) and chiral ($n=7, m=1,2,3,\dots,6$) geometry of various chirality and compared with those for carbon nanotubes.

Figure 2 giving the variation of the enthalpies of formation/atom of the carbon and boron nitrogen nanotubes, shows that thermodynamic stabilization depends on the chiral vector, n . It is noteworthy to mention that the boron nitride nanotubes are thermodynamically stabilized with the increasing of the chiral vector, n . We got similar conclusions for tubes with armchair and chiral geometry, figures 3 and 4. These studies suggest that all BN nanotubes are thermodynamically more stable than their carbon analogues.

In order to check the validity of these trends, ab initio RHF/3-21G calculations have been carried out on the AM1 optimized geometries of (5,5), (10,0), (7,3)BN nanotubes. The results confirm that the (5,5)BN tube is more stable than the (7,3)BN (with 258.41kcal/mol) and (10,0)BN nanotube (with 501.95kcal/mol), respectively.

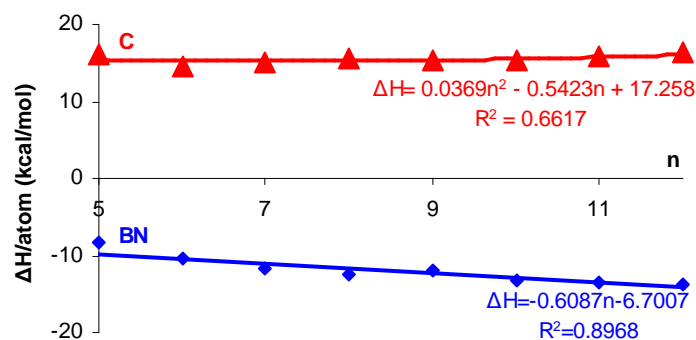


Figure 2. Enthalpy of formation (per atom) as a function of the chiral vector n for $(n,0)$ C/BN nanotubes with $n=5, 6, \dots, 14$.

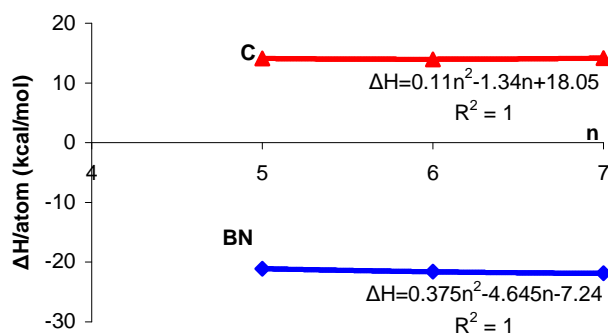


Figure 3. Enthalpy of formation (per atom) as a function of the chiral vector n for (n,n) C/BN nanotubes with $n=5, 6, 7$.

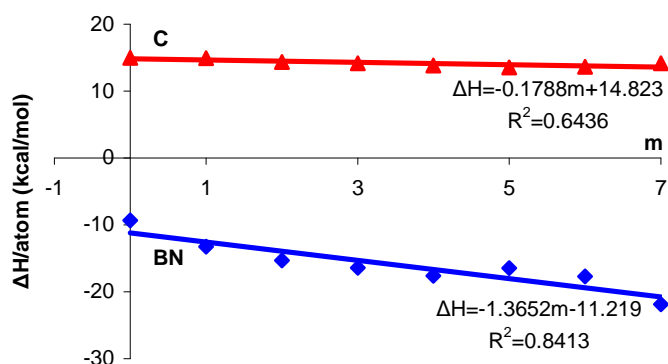


Figure 4. Enthalpy of formation (per atom) as a function of the chiral vector m for $(7,m)$ C/BN nanotubes with $m = 0, \dots, 7$.

The above-mentioned reasons, motivated us to study the possible defects of the BN nanotubes that might stabilize the zigzag and chiral geometry.

B) The influence of possible defects of the BN nanotubes

In the synthesis of BN nanotubes, different kinds of defects due to the deviation from the 1:1 stoichiometry or to the presence of other elements like carbon or aluminum may appear in their structure. We analyzed these influences on energetic and electronic properties of the tubes. For this, we substituted two atoms of nitrogen located at the tip edges of the tubules with boron, carbon or aluminum, figure 5.

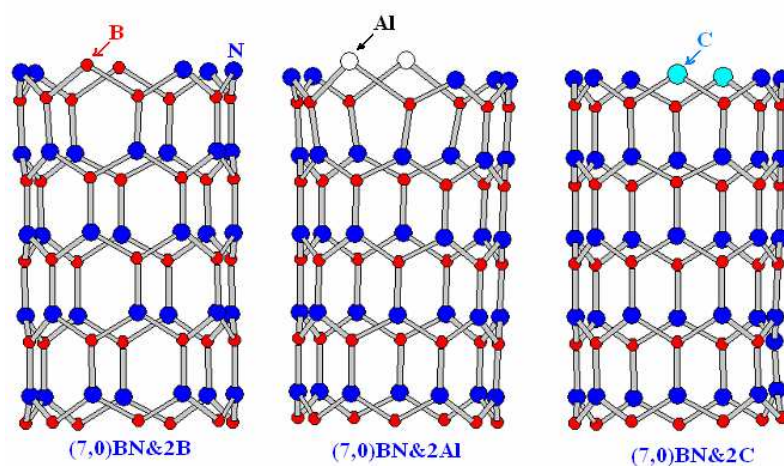


Figure 5. Structural models of doped boron nitride nanotube ($L=4$).

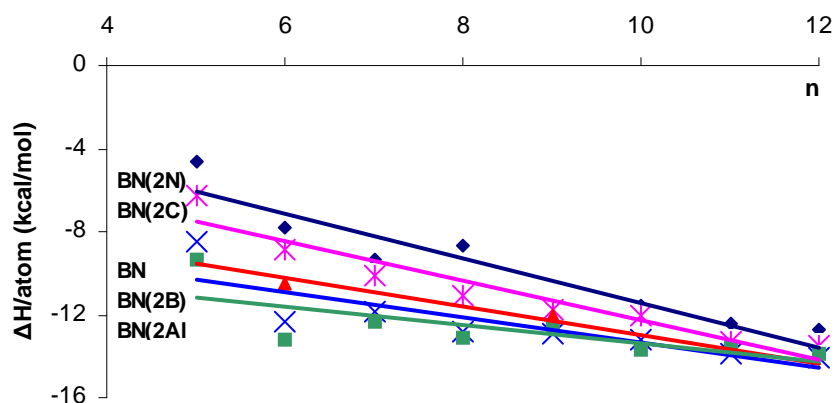


Figure 6. Enthalpy of formation (per atom) as a function of the chiral vector n for the doped $(n,0)$ BN nanotubes with $n=5,6,\dots,14$. Display equations and R-square values on chart:

$$\begin{aligned}
 \text{BN(2N): } \Delta H &= -1.0671n - 0.7518; & R^2 &= 0.8845 \\
 \text{BN(2C): } \Delta H &= -0.9481n - 2.8187; & R^2 &= 0.915 \\
 \text{BN: } \Delta H &= -0.6835n - 6.1419; & R^2 &= 0.8659 \\
 \text{BN(2B): } \Delta H &= -0.6079n - 7.2857; & R^2 &= 0.7101 \\
 \text{BN(2Al): } \Delta H &= -0.4486n - 8.9121; & R^2 &= 0.5618.
 \end{aligned}$$

Graph 6 shows comparatively the stability of the BN tubes for different doping atoms. Boron and aluminium doping stabilises the zigzag BN nanotubes while carbon or an excess of nitrogen leads to instability of the tubes. Chiral BN nanotubes are stabilizes only by aluminium, figure 7. In contrary to these, the presence of any dopant conducts to instability of the armchair tubes, figure 8.

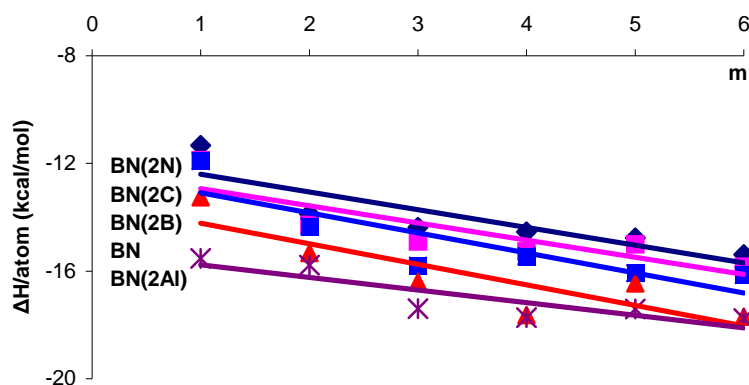


Figure 7. Enthalpy of formation (per atom) as a function of the chiral vector m for the doped $(7, m)$ BN nanotubes with $m=1, \dots, 6$. Display equations and R-square values on chart:

$$\begin{aligned}
 \text{BN(2N): } \Delta H &= -0.6597m - 11.736; & R^2 &= 0.7573 \\
 \text{BN(2C): } \Delta H &= -0.638m - 12.295; & R^2 &= 0.7339 \\
 \text{BN(2B): } \Delta H &= -0.7449m - 12.348; & R^2 &= 0.7299 \\
 \text{BN: } \Delta H &= -0.7646m - 13.454; & R^2 &= 0.7441 \\
 \text{BN(2Al): } \Delta H &= -0.4691m - 15.295; & R^2 &= 0.7583.
 \end{aligned}$$

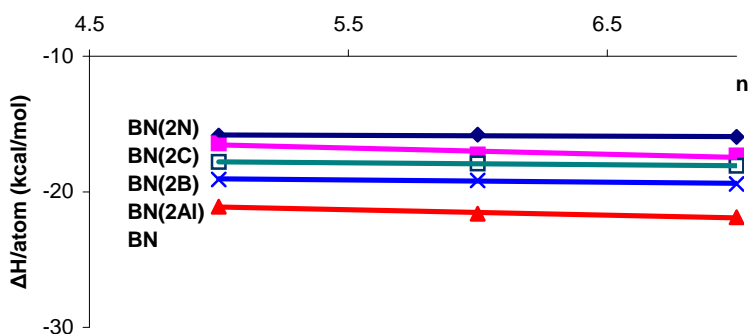


Figure 8. Enthalpy of formation (per atom) as a function of the chiral vector n for the doped (n, n) BN nanotubes with $n=5, 6, 7$. Display equations and R-square values on chart:

$$\begin{aligned}
 \text{BN(2N): } \Delta H &= -0.05n - 15.57; & R^2 &= 0.3425 \\
 \text{BN(2C): } \Delta H &= -0.45n - 14.3; & R^2 &= 0.8242 \\
 \text{BN(2B): } \Delta H &= -0.145n - 17.057; & R^2 &= 0.9902 \\
 \text{BN(2Al): } \Delta H &= -0.165n - 18.227; & R^2 &= 0.9187 \\
 \text{BN: } \Delta H &= -0.395n - 19.157; & R^2 &= 0.9677.
 \end{aligned}$$

Table 1.Calculations of the $E_{\text{HOMO}}-E_{\text{LUMO}}$ for doped BN nanotubes.

tube	$E_{\text{HOMO}}-E_{\text{LUMO}}$ (eV)				
	BN(2C)	BN(2Al)	BN(2B)	BN(2N)	BN
(5, 0)	4.49	4.28	4.68	4.69	5.57
(6, 0)	4.5	4.45	4.7	5.09	5.37
(7, 0)	4.79	4.74	5.04	5.25	5.66
(8, 0)	4.67	5.03	4.97	5.28	5.59
(9, 0)	4.57	5.18	5.1	5.97	5.59
(10, 0)	4.32	5.33	5.58	5.3	5.57
(11, 0)	4.4	4.9	5.02	5.4	5.5
(12, 0)	4.5	5.2	5.45	5.52	5.61
(13, 0)	4.6	5.3	5.3	5.5	5.7
(14, 0)	4.7	5.1	5.4	5.6	5.4
(5, 5)	2.68	6.51	8.09	8.27	8.67
(6, 6)	1.92	6.5	8.16	8.24	8.66
(7, 7)	4.73	6.59	5.52	8.49	8.66
(7, 1)	4.64	5.4	4.3	4.96	4.01
(7, 2)	4.72	4.44	5.14	4.86	5.58
(7, 3)	1.81	4	4.64	4.15	4.28
(7, 4)	3	4.1	4.5	4.7	4.92
(7, 5)	2.7	4	4.25	4.5	4.7
(7, 6)	3.84	3.9	4	4.35	4.5

The possible defects of the BN nanotubes lead to small values of their energies gap ($E_{\text{HOMO}}-E_{\text{LUMO}}$), table 1, so the kinetic stability is lower compared to the corresponding pure analogues.

C) Electronic properties of the pure/doped BN nanotubes

The effect of chirality and length of the tube

The fact that the electronic properties of the carbon nanotubes depend upon their chirality and diameter makes them unsuitable for use in some electronic devices.

One of the current research topics in this area is the influence of different chiralities and lengths of the BN tubes on electronic properties for possible applications on nanodevices (actuators³⁰, nanoscale diodes^{31, 32}). We calculated the electronic properties of zigzag ($n=5, \dots, 9$), armchair ($n=5, 6, 7$) and chiral ($n=5, m=1, 2, 3$) BN nanotubes.

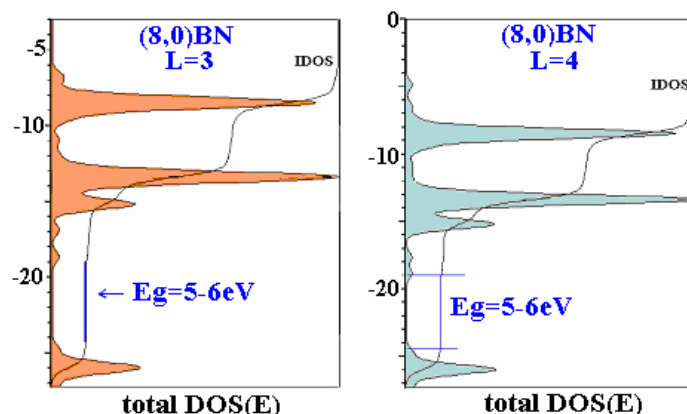


Figure 9. The total DOS(E) and IDOS plots of the zigzag BN nanotubes.

The results obtained for (8,0)BN nanotubes with $L=3$ and 4 are revealed in figure 9. From the DOS(E) plots it is obvious that the lowest bands (valence band) are composed of N(2s) derived states and the conduction bands consist of N(2p) and B(2s, 2p) derived states.

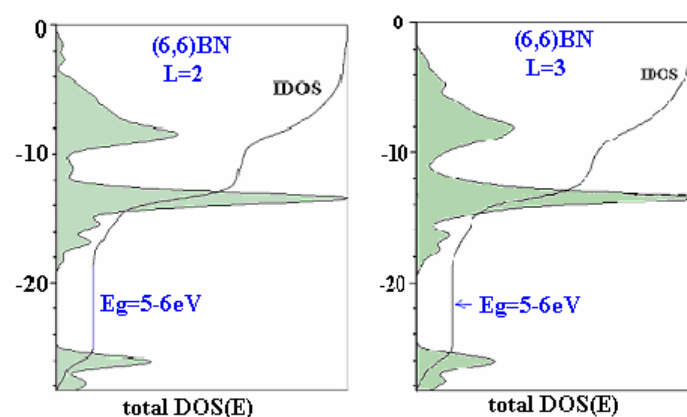


Figure 10. The total DOS(E) and IDOS plots of the armchair BN nanotubes.

An important aspect of this section is that all zigzag tubes can exhibit an insulating behavior (figure 9). Similar conclusions are derived from figure 10 for armchair nanotubes, in agreement with the predictions of Blasé¹⁹.

The total DOS for (5,3)BN nanotube with $L=3$ and 4 is shown in figure 11. From the DOS(E) plots it is clear that the long tube ($L=4$) is a semiconductor while the short tube ($L=3$) have an insulator character. It is also important to notice that the chiral tubes can behave either as a semiconductor or as an insulator dependent on chirality, diameter or length of the tube.

Consequently, these simple studies provide evidence for possible applications of the armchair and zigzag BN nanotubes on nanodevices.

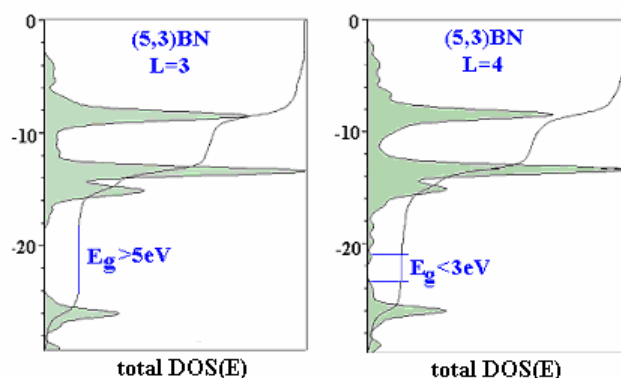


Figure 11. The total DOS(E) and IDOS diagrams of the chiral BN nanotubes.

The influence of possible defects of the BN nanotubes

In case of doping with boron, nitrogen and aluminum, the electronic states near the forbidden bands displays gap energies of 5-6eV independent on the geometry of the tube. Thus, the lowest bands are composed of N (2s) derived states and the highest band of N(2p), B(2s, 2p) and Al(3s, 3p) contributions, figure 12. The valence bands are slightly affected by metal intercalation.

The Fermi level is located in the middle of Van Hove singularities corresponding to N p-orbital derived states. This is considered an indication [33] that there is overlap with boron and aluminium s, p-orbital. The gap energy of 5eV implies insulator properties.

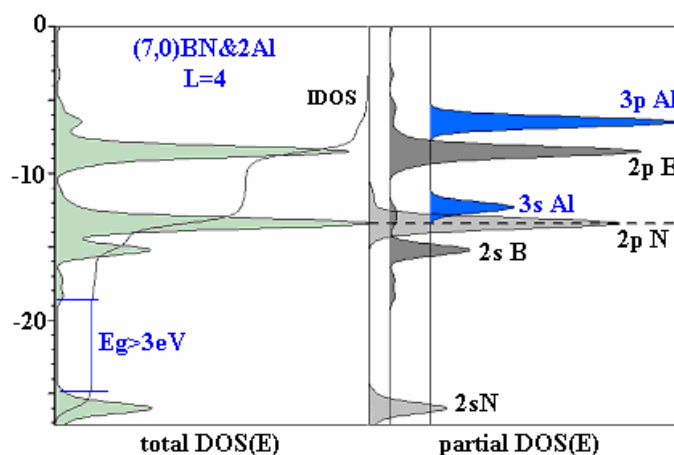


Figure 12. The partial, total DOS(E) and IDOS plots for (7,0)BN&2Al nanotube.

Doping the BN tube with carbon changes the electronic properties of the zigzag and chiral tube by new bands (Figure 13a,b). This bands correspond to an acceptor level in semiconductors with very low dopant concentration, so that both gap energies are smaller than 3eV and the tube became semiconductors.

Defects brought by deviations from the 1:1 stoichiometry or by the presence of aluminium lead to slight tube-impurities interactions and insignificant modification of the electronic properties. By contrast, doping with carbon decreases the energy gap until a semiconductor behavior.

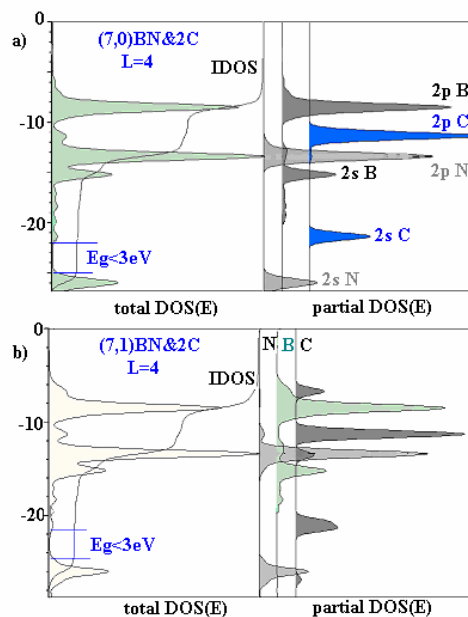


Figure 13. The total DOS and IDOS plots of the (7,0) and (7,1)BN&2C nanotube. The N(2s, 2p), B(2s, 2p) and C(2s, 2p) contributions to the DOS are projected.

Interestingly, the chiral BN nanotubes can behave either as a semiconductor or as an insulator and only changing their structure (chirality, length) controls their band gap.

The armchair and zigzag BN nanotubes may also be suitable for electronic devices because they have a constant band gap around 5-6 eV independent of their radius, chirality, length and different kinds of defects due to the deviation from the 1:1 stoichiometry or the presence other elements like aluminium.

Conclusion

All BN nanotubes are thermodynamically more stable relative to their carbon analogues. The armchair BN tubes are more stable than the chiral and zigzag nanotubes, respectively. The thermodynamic stability of the zigzag BN nanotubes can be enhanced by adding aluminium or boron while the chiral tubes can be stabilized by adding only aluminium.

The zigzag and armchair BN nanotubes possess a band gap of 5-6 eV independent of the chirality, length of tube and defects types. In contrast, the energy gaps of the chiral BN tubes can be controlled only by changing their structure. Note also that boron, nitrogen and aluminum doping modifies insignificantly the electronic properties of the BN nanotubes whereas carbon atoms diminish the energy gap until a semiconductor behavior.

Acknowledgements. We thank Prof. G. Calzaferri for the access to the BICON-CEDIT packages of programs.

REFERENCES

1. S. Iijima, *Nature*, **1991**, 354, 56.
2. N. Hamada, S. Sawada, A. Oshiyama, *Phys. Rev. Lett.*, **1992**, 68, 1579.
3. A. Hassanien, M. Tokumoto, Y. Humazawa, H. Kataura, Y. Maniwa, S. Suzuki, Y. Achiba, *Appl. Phys. Lett.*, **1998**, 73, 3839.
4. A. Hassanien, M. Tokumoto, S. Ohshima, Y. Kuriki, F. Ikazaki, K. Uchida, M. Yumura, *Appl. Phys. Lett.*, **1999**, 75, 2755.
5. R. Saito, M. Fujita, G. Dresselhaus, M. S. Dresselhaus, *Appl. Phys. Lett.*, **1992**, 60, 2204.
6. N. Hamada, S. Sawada, A. Oshiyama, *Phys. Rev. Lett.*, **1992**, 68, 1579.
7. X. Blasé, A. Rubio, S. G. Louie, M. L. Cohen, *Europhys. Lett.*, **1994**, 28, 335.
8. X. Blasé, J. C. Charlier, A. De Vita, R. Car, *Appl. Phys. Lett.*, **1997**, 70, 197.
9. D. L. Carroll, P. Redlich, X. Blasé, J. C. Charlier, S. Curran, P. M. Ajayan, S. Roth, M. Ruthle, *Phys. Rev. Lett.*, **1998**, 81, 2332.
10. R. Czerw, M. Terrones, J. C. Charlier, X. Blasé, B. Foley, R. Kamalakaran, N. Grobert, H. Terrones, D. Tekleab, P. M. Ajayan, W. Blau, M. Ruhle, D. L. Carroll, *Nano Lett.*, **2001**, 1, 457.
11. J. C. Charlier, M. Terrones, M. Baxendale, V. Meunier, T. Zacharia, N. L. Rupasinghe, W. K. Hsu, N. Grobert, H. Terrones, G. A. J. Amaratunga, *Nano Lett.*, **2002**, 2, 1191.
12. G. Calzaferri, R. Rytz, *J. Phys. Chem.*, **1995**, 99, 12141.
13. J. O. Lu, *Phys. Rev. Lett.*, **1995**, 74, 1123.
14. A. Rubio, Y. Miyamoto, X. Blasé, M. L. Cohen, S. G. Louie, *Phys. Rev.*, **1996**, 53B, 4023.
15. J. Zhao, J. Han, J. P. Lu, *Phys. Rev.*, **2002**, 65B, 193401.
16. N. C. Greenham, R. H. Friend, *Solid State Physics, Advances in Research and Application*, edited by H. Ehrenreich and F. Spaepen, **1995**, 49, 1, Academic Press, New York.
17. C. Dekker, *Physics Today*, **1999**, may, 22.
18. J. Kongsted, A. Osted, L. Jensen, P. O. Astrand, K. V. Mikkelsen, *J. Phys. Chem.*, **2001**, 105 B, 10243.
19. X. Blasé, J. C. Charlier, A. De Vita, R. Car, *Appl. Phys. (Materials-Science-Processing)*, **1999**, 68 A, 293.
20. K. Gofron, H. Ding, C. Gu, R. Liu, B. Dabrowski, B. Veal, W. Cramer, G. Jennings, *J. Phys. Chem. Solids*, **1993**, 54, 1193.
21. N. L. Allinger, *J. Am. Chem. Soc.*, **1977**, 99, 8127.
22. J. J. P. Stewart, *QCPE Bulletin*, **1989**, 9, 80.
23. M. J. S. Dewar, E. G. Zoebisch, E. F. Healy, J. J. P. Stewart, *J. Am. Chem. Soc.*, **1985**, 107, 3902.
24. *HyperChem*, release 4.5 for SGI, 1991-1995, HyperCube, Inc.
25. *Spartan'02*, Wavefunction, Inc., Irvine, C.A.
26. M. Brandle, R. Rytz, G. Calzaferri, *BICON-CEDIT – manual*, Bern, **1997**.
27. N. Hamada, S. Sawada, a. Oshiyama, *Phys. Rev. Lett.*, **1992**, 68, 1579.
28. Ş. Erkoc and S. Ozkaymak, *Eur. Phys. J.*, **1998**, 4D, 331.
29. S. Weber, <http://www.icystal.com/steffenweber/JAVA/jnano/jnano.html>, 2000.
30. K. H. Baughman, C. Cui, A. A. Zakhidov, Z. Iqbal, J.N. Baricci, G. M. Spinks, G. G. Wallace, A. Mazzoldi, D. De Rosi, A. G. Rinzier, O. Jaschinski, S. Roth, M. Kertesz, *Science*, **1999**, 284, 1340.
31. S. F. Bent, *Conference 2003: Novel Electronic Materials*, Stanford.
32. P.E. Lammert, V. H. Crespi, A. Rubio, *Phys. Rev. Lett.*, **1999**, 299, 368.
33. E. Cappelluti, L. Pietronero, *Europhys. Chem.*, **1996**, 36, 619.